An Investigation of Hall Propulsor Characteristics

H E Brandmaier,* J L Durand,† M C Gourdine,‡ and A Rubel§
Curtiss-Wright Corporation, Wood-Ridge, N J

The steady, one-dimensional, inviscid magnetogasdynamic flow equations are derived for the coaxial, constant area, Hall propulsor using a slightly ionized plasma For the case of a radial magnetic field and axial electric field, flow regimes are established for which supersonic acceleration combined with an increasing axial Mach number is possible These are functions of the ratio of the Hall parameter to one plus the "ion slip" parameter, designated as tanϕ, Mach number, and a nondimensional quantity involving the axial and azimuthal plasma velocities and the electric and magnetic field strengths For each value of tanϕ there is a maximum attainable axial Mach number It is further shown that for large tanϕ the maximum final velocity is just $\gamma/(\gamma - 1)$ times the initial velocity or, for $\gamma = \frac{5}{3}$, (V max/V initial) = 2 5 This velocity can be increased by staging in such a manner that the maximum Mach number is approached, thereby minimizing the over-all static temperature rise through the propulsor An experimental model was designed and fabricated to verify the predictions of the analytical investigation Experimentation is currently being conducted using a radio frequency generated plasma

Nomenclature

A = area
B = magnetic flux density ~ weber/m^2
b = ion slip parameter
E = electric field intensity
f = fraction of atoms not ionized
g = gravitational constant
h_T = total enthalpy
I = current
J = current density
L = reference length
M = Mach number, molecular weight
m = mass flow rate per unit flow area
N = $\sigma B^2 L/m(1 + b)$
P = pressure ~ torr
P = probability of collision as given by Ref 18
Q = cross section ~ Å^2
R = gas constant
r = radial coordinate
S = $S_z/(1 - S_\theta)$
$S_{z\,\theta}$ = nondimensional velocity, $V_{\theta}B/E$
T = temperature ~ °K
U = energy ~ ev
V = velocity
z = axial coordinate
α = $\tan^{-1}(B_z/B_r)$
β = $\tan^{-1}(E_z/E_r)$
γ = specific heat ratio
η = energy conversion efficiency
μ = magnetic permeability
θ = azimuthal coordinate
ρ = mass density
σ = electrical conductivity, rigid sphere diameter ~ Å
τ = time between collisions
ϕ = $\tan^{-1}\omega_e\tau_e/(1 + b)$
ω = cyclotron frequency

Subscripts

a = atom
e = electron
i = ion
0 = channel inlet value
r = radial direction
z = axial direction
θ = azimuthal direction
ea = electron-atom collision
ia = ion-atom collision

Received December 2, 1962; revision received January 24, 1964

* Chief Project Engineer, Wright Aeronautical Division
† Project Engineer, Wright Aeronautical Division Member AIAA
‡ Chief Scientist, Wright Aeronautical Division Member AIAA
§ Assistant Project Engineer, Wright Aeronautical Division Member AIAA

Introduction

THE comparative performance of electrical propulsors can be expressed in terms of conversion efficiency as a function of specific impulse Theoretical values for the hydrogen arcjet,[1] the mercury bombardment,[2] and cesium contact[3] ion engines are shown in Fig 1 Between approximately 1100 and 4000 sec, the efficiencies of these propulsors are less than 50% This specific impulse range is generally considered to be the region of application of steady-flow magnetogasdynamic (MGD) propulsors

Steady-flow MGD propulsors of both the Faraday and Hall types are currently being investigated [4] In the former, the accelerating, or $\mathbf{J} \times \mathbf{B}$, force results from the interaction of orthogonal electric and magnetic fields applied externally to a rectangular channel If the ratio of electron cyclotron frequency to mean collision frequency of electrons with neutrals and ions exceeds one, because of large magnetic fields and/or low particle densities, axial Hall currents become significant These interact with the applied magnetic field, producing undesirable transverse forces and thereby reduced performance [5] Axial segmentation of the electrodes[6] serves to reduce or eliminate the Hall current An alternate approach is to use the Hall current directly to produce an axial accelerating force in an annular channel This was suggested and initially investigated by Hess et al [7–9]

Three possible Hall propulsor field configurations are shown schematically in Fig 2 In Fig 2a the radial electric field and axial component of the magnetic field induce an azimuthal Hall current This current interacts with the radial component of the magnetic field, resulting in an axial accelerating force Unfortunately, as in the Faraday propulsor, an axial current is also induced which leads to poor performance An oversimplified analysis by the present authors[10] yielded a maximum conversion efficiency of 10% for a slightly ionized plasma Segmenting the electrodes,[8 9] as shown in Fig 2b, suppresses this axial current by establishing an axial electric field On the same basis the con-

version efficiency increased to 65% Alternatively, a purely radial magnetic field coupled to an axial electric field produces the same result This is shown in Fig 2c

In the following sections a detailed analysis of the Hall propulsor with radial magnetic and axial electric fields (Fig 2c) is presented The main objective was the development and solution of a one-dimensional set of differential equations, representing the gasdynamic conservation laws, which is consistent with Maxwell's equations As will be demonstrated, these equations are similar to the one-dimensional equations presented by Shapiro for purely gasdynamic channel flow[11] and by Yoler[12] and Sears,[13] for example, for Faraday-type magnetogasdynamic channel flow Thus, this investigation differs from previous Hall device studies,[4 7-9] which were restricted to derivations of expressions for local flow properties, propulsive force, and efficiency A slightly ionized gas is assumed throughout the analysis Excellent discussions of the Hall current ion accelerator, which employs a fully ionized gas, have been given by Hess[14] and Ellis [15]

Basic Equations

The magnetogasdynamic (MGD) characteristics of the Hall propulsor were determined from the solution of the following equations:

Mass Conservation

$$\nabla \rho\mathbf{V} = 0 \tag{1}$$

Momentum Conservation

$$\rho\mathbf{V}\,\nabla\mathbf{V} + \nabla P - \mathbf{J} \times \mathbf{B} = 0 \tag{2}$$

Energy Conservation

$$\rho\mathbf{V}\,\nabla[\tfrac{1}{2}V^2 + (\gamma/\gamma - 1)RT] - \mathbf{E}\,\mathbf{J} = 0 \tag{3}$$

Equation of State

$$P = \rho RT \tag{4}$$

Implicit in these equations are the following assumptions: 1) steady, continuum flow; 2) electrically neutral, ideal, slightly ionized, three-species gas mixture; 3) constant fluid properties; 4) negligible shear and gravitational forces; and 5) no heat transfer through channel walls

The relation between current density and electric field was supplied by Ohm's law, as derived by Cowling [16] Neglecting electron partial pressure gradients and assuming a small ratio of ion cyclotron to ion-neutral collision frequency compared to the corresponding ratio for electrons, Ohm's law can be expressed as

$$\mathbf{J} = \frac{\sigma(1+b)}{(1+b)^2 + (\omega\bar{\tau})^2}\left\{\left[\mathbf{E}' - \left(\mathbf{E}'\frac{\mathbf{B}}{B}\right)\frac{\mathbf{B}}{B}\right] - \left(\frac{\omega\bar{\tau}_e}{1+b}\right)\mathbf{E}' \times \frac{\mathbf{B}}{B}\right\} + \sigma\left(\mathbf{E}'\frac{\mathbf{B}}{B}\right)\frac{\mathbf{B}}{B} \tag{5}$$

where

$$\mathbf{E}' = \mathbf{E} + \mathbf{V} \times \mathbf{B} \tag{6}$$

The Hall effect is embodied in the parameter $\omega\bar{\tau}$, the ratio of electron cyclotron frequency to the mean collision frequency of electrons with neutrals and ions The effect of the ratio of ion cyclotron frequency to ion-neutral collision frequency is contained in b, referred to as the "ion slip" parameter, which is defined as

$$b = 2f^2\omega_{ia}\tau_{ia}\omega\,\bar{\tau}_e \tag{7}$$

For the slightly ionized plasmas considered in this analysis, $f \approx 1$

In addition to Eqs (1-5), charge conservation requires that

$$\nabla\,\mathbf{J} = 0 \tag{8}$$

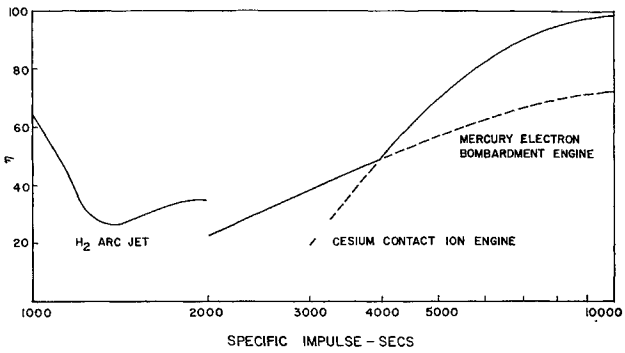

Fig 1 Estimated conversion efficiencies of arcjet and ion engines as functions of specific impulse

Finally, Maxwell's electromagnetic equations are, at steady state, the following:

Ampere's Law

$$\nabla \times \mathbf{B} = \mu\mathbf{J} \tag{9}$$

Faraday's Law

$$\nabla \times \mathbf{E} = 0 \tag{10}$$

Gauss' Law

$$\nabla\,\mathbf{B} = 0 \tag{11}$$

One-Dimensional Magnetogasdynamic Equations

With the objective of reducing these equations to a form similar to that for one-dimensional flow in a Faraday device,[12] additional assumptions were required These are as follows: 1) small axial area variations such that the radial velocity component can be neglected; 2) axisymmetric flow, $\partial(\ )/\partial\theta = 0$; 3) negligible radial variations of flow parameters, $\partial(\ )/\partial r = 0$ (this implies flow in an annular channel whose height is small compared to its mean radius); 4) negligible end effects; and 5) negligible induced magnetic fields, $\nabla \times \mathbf{B} = 0$

For compactness, the vector components of **E** and **B** were expressed trigonometrically using the angles shown in Fig 2b Thus, from Eqs (5) and (6), the current density com-

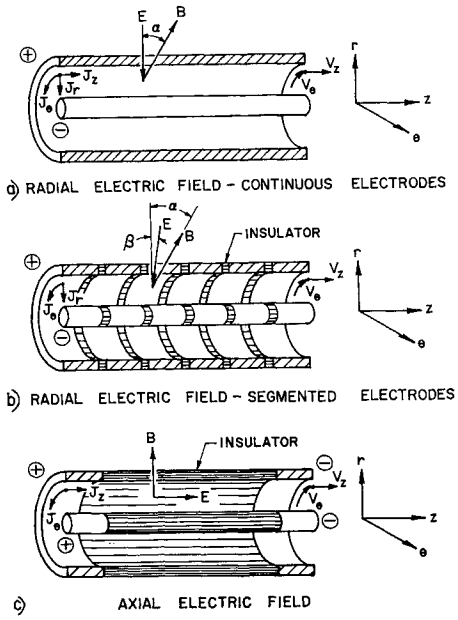

Fig 2 Hall propulsor electric and magnetic field configurations

ponents are

$$J = \frac{\sigma E \cos^2\phi \sin\alpha}{1+b}\{[\sin(\alpha-\beta)+S_\theta] - \tan\phi S\ \cos\alpha\} + \sigma E \cos(\alpha-\beta)\cos\alpha \quad (12)$$

$$J_\theta = \frac{\sigma E \cos^2\phi}{1+b}\{\tan\phi[\sin(\alpha-\beta)+S_\theta] + S\ \cos\alpha\} \quad (13)$$

$$J = \frac{-\sigma E \cos^2\phi \cos\alpha}{1+b}\{[\sin(\alpha-\beta)+S_\theta] - \tan\phi S\ \cos\alpha\} + \sigma E \cos(\alpha-\beta)\sin\alpha \quad (14)$$

where

$$S = \frac{VB}{E} \qquad S_\theta = \frac{V_\theta B}{E} \qquad \tan\phi = \frac{\omega_e \bar{\tau}_e}{1+b}$$

are dimensionless flow parameters

Inserting Eqs (12–14) into Eqs (1–3) yielded

$$\rho V = m \quad (15)$$

$$\frac{B}{E}\frac{d}{dz'}V_\theta + \frac{\sigma B^2 L \cos^2\phi}{(1+b)m}\{[\sin(\alpha-\beta)+S_\theta] - \tan\phi S\ \cos\alpha\} = 0 \quad (16)$$

$$\frac{d}{dz'}V + \frac{1}{m}\frac{d}{dz'}P - \frac{\sigma EBL\cos^2\phi\cos\alpha}{(1+b)m} \times \{\tan\phi[\sin(\alpha-\beta)+S_\theta] + S\ \cos\alpha\} = 0 \quad (17)$$

where z' is the axial coordinate nondimensionalized by the propulsor length, and

$$\frac{d}{dz'}h_T - \frac{\sigma E^2 L\cos^2\phi}{(1+b)m}\sin(\alpha-\beta)\{[\sin(\alpha-\beta)+S_\theta] - \tan\phi S\ \cos\alpha\} - \frac{\sigma E^2 L}{m}\cos^2(\alpha-\beta) = 0 \quad (18)$$

where

$$h_T = \tfrac{1}{2}V_\theta^2 + \tfrac{1}{2}V^2 + [\gamma/(\gamma-1)]RT \quad (19)$$

The pressure gradient term in Eq (17) was eliminated using the equations of state, Eq (4), and mass conservation, Eq (15), in differential form Thus,

$$\frac{1}{P}\frac{d}{dz}P + \frac{1}{V}\frac{d}{dz}V + \frac{1}{A}\frac{d}{dz}A - \frac{1}{T}\frac{d}{dz}T = 0 \quad (20)$$

Substituting $(d/dz)T$ from Eqs (18) and (19) into Eq (20) and the result into Eq (17) along with the definition of Mach number gave, after using Eq (16) to eliminate the (d/dz) V_θ term,

$$\frac{1}{V_z}\frac{d}{dz'}V_z = \frac{1}{M^2-1}\left\{\frac{1}{A}\frac{dA}{dz} - \gamma\frac{\sigma B^2 L\cos^2\phi}{(1+b)m}\left(\frac{M_z}{S}\right)^2 \times \left[(S_z\cos\alpha)^2 + \frac{1}{\gamma}\tan\phi[\sin(\alpha-\beta)+S_\theta]S_z\cos\alpha + \frac{\gamma-1}{\gamma}[\sin(\alpha-\beta)+S_\theta]^2 + \frac{\gamma-1}{\gamma}(1+b)\times\frac{\cos^2(\alpha-\beta)}{\cos^2\phi}\right]\right\} \quad (21)$$

where M_z is the Mach number based on V For acceleration by electromagnetic forces, the bracketed term must be negative for supersonic flow and positive for subsonic flow This requires that

$$[\sin(\alpha-\beta)+S_\theta]\cos\alpha < 0 \quad (22)$$

for supersonic flow

The purely radial magnetic field and axial electric field in Fig 2c $\alpha = 0$ and $\beta = \pi/2$, satisfy this condition when $S_\theta < 1$ Reversing the magnetic field, $\alpha = \pi$ also produces acceleration In this case $S_\theta > -1$, since V_θ changes direction as can be seen from Eq (16) In both cases, from Eq (18), the stagnation enthalpy increases, since energy is removed from the electric field The radial electric field cases can be analyzed in a similar fashion

The differential equation for axial Mach number was obtained from the definition for M in differential form:

$$\frac{1}{M}\frac{d}{dz}M = \frac{1}{V}\frac{d}{dz}V - \frac{1}{2T}\frac{d}{dz}T \quad (23)$$

Substituting Eqs (16, 18, 19, and 21) into (23) yielded

$$\frac{1}{Mz}\frac{d}{dz'}M_z = \frac{1+[(\gamma-1)/2]M^2}{M^2-1}\left\{\frac{1}{A}\frac{d}{dz'}A - \gamma N\frac{A}{A_0}\times\cos^2\phi\left(\frac{Mz}{S}\right)^2\left[(S\ \cos\alpha)^2 + \frac{(\gamma+1)/2\gamma}{1+[(\gamma-1)/2]M^2}\tan\phi\times[\sin(\alpha-\beta)+S_\theta]S\ \cos\alpha + \left(\frac{\gamma-1}{2\gamma}\right)\frac{\gamma M^2+1}{1+[(\gamma-1)/2]M^2}\times\left([\sin(\phi-\beta)+S_\theta]^2 + (1+b)\frac{\cos^2(\alpha-\beta)}{\cos^2\phi}\right)\right]\right\} \quad (24)$$

where N is a magnetic interaction parameter defined by

$$N = \sigma B^2 L/(1+b)m_0 \quad (25)$$

Although not required for the determination of the flow properties, the differential expressions for static pressure and temperature are

$$\frac{1}{P}\frac{dP}{dz'} = \frac{-\gamma M_z^2}{M^2-1}\left\{\frac{1}{A}\frac{d}{dz'}A - \gamma N\frac{A}{A_0}\cos^2\phi\left(\frac{M_z}{S}\right)^2\times\left[\frac{1+(\gamma-1)M_z^2}{\gamma M^2}(S\ \cos\alpha)^2 + \frac{\tan\phi}{\gamma M^2}[\sin(\alpha-\beta)+S_\theta]S\times\cos\alpha + \left(\frac{\gamma-1}{\gamma}\right)\left([\sin(\alpha-\beta)+S_\theta]^2 + \frac{(1+b)}{\cos^2\phi}\cos^2(\alpha-\beta)\right)\right]\right\} \quad (26)$$

$$\frac{1}{T}\frac{d}{dz'}T = -\frac{(\gamma-1)M_z^2}{M^2-1}\left\{\frac{1}{A}\frac{d}{dz'}A - \gamma N\frac{A}{A_0}\cos^2\phi\left(\frac{M_z}{S}\right)^2\times\left[(S\ \cos\alpha)^2 + \frac{\tan\phi}{\gamma M^2}[\sin(\alpha-\beta)+S_\theta]S_z\cos\alpha + \frac{(\gamma M_z^2-1)}{\gamma M^2}\left([\sin(\alpha-\beta)+S_\theta]^2 + \frac{(1+b)}{\cos^2\phi}\cos^2(\alpha-\beta)\right)\right]\right\} \quad (27)$$

Satisfaction of Maxwell's Equations

The numerical solution of Eqs (16, 21, and 24) for the magnetogasdynamic flow properties depends on the variation of the electric and magnetic fields within the channel This information was obtained from Maxwell's relations, Eqs (9) and (10), consistent with the assumptions of this analysis For $\nabla \times \mathbf{B} = 0$, either $\mathbf{B}$ = const or Bz must exist (in the Fig 2c case) and vary radially to balance the axial variation of Br Similarly, from $\nabla\ \mathbf{B} = 0$, Br must vary radially to balance the axial variation of Bz However, for small magnetic field variations, these two-dimensional effects are also small For the remainder of this study, it was assumed that Br = const

Similarly, from $\nabla \times \mathbf{E} = 0$ it followed that the radial electric field, in Figs 2a and 2b, is approximately constant along the channel Inserting Ohm's law [Eq (5)] into

charge conservation [Eq (8)] gave, for constant magnetic field,

$$\nabla \mathbf{J} = \frac{\sigma \cos^2\phi}{1+b}\left\{\nabla(\mathbf{E}+\mathbf{V}\times\mathbf{B}) - \frac{\mathbf{B}}{B}\nabla\left(\mathbf{E}\frac{\mathbf{B}}{B}\right) - \tan\phi\left[\frac{\mathbf{B}}{B}\nabla(\mathbf{V}\,\mathbf{B}) - B\nabla\mathbf{V}\right]\right\} + \sigma\frac{\mathbf{B}}{B}\nabla\left(\mathbf{E}\frac{\mathbf{B}}{B}\right) = 0 \quad (28)$$

Performing the indicated operations yielded $(d/dz)J_z = 0$ or $J = \text{const}$ Thus, in the case of a radial electric field with continuous electrodes (Fig 2a), charge conservation cannot be satisfied in a one-dimensional model, since $E = 0$ In the cases of a radial electric field with segmented electrodes (Fig 2b) and an axial electric field (Fig 2c), it is satisfied The limit for the Fig 2b configuration, considered by Hess et al ,[8,9] which yields optimum performance is $J = 0$ To the same degree of approximation that flow in a variable area channel can be studied using a one-dimensional model, the constant axial current density condition can be replaced by a constant axial current, or $I = \int J\,dA = \text{const}$

Simplification for Axial Electric Field and Radial Magnetic Field

The system of equations governing flow in a Hall propulsor with an axial electric field ($\beta = \pi/2$) and a radial magnetic field ($\alpha = 0$) (Fig 2c) was reduced to the following form To determine the significant flow properties without excessive complications, a constant area channel was assumed Thus,

$$S\frac{d}{dz'}S = -\gamma N\cos^2\phi\frac{M_z^2}{M^2-1}\left[S^2 - \frac{1}{\gamma}\tan\phi S + \frac{\gamma-1}{\gamma}\right]\times(1+\tan\phi S) \quad (29)$$

$$\frac{1}{M}\frac{d}{dz'}M_z = -\gamma N\cos^2\phi\frac{M_z^2}{M_z^2-1}\left[\left(1+\frac{\gamma-1}{2}M^2\right) - \frac{\gamma+1}{2\gamma}\tan\phi\frac{1}{S} + \frac{\gamma-1}{2\gamma}(1+\gamma M^2)\frac{1}{S^2}\right] \quad (30)$$

These relations were obtained from Eqs (16, 21, and 24) using Eq (14) with $J = \text{const}$ The dependent variables are axial Mach number and the parameter S, defined as

$$S = S/(1-S_\theta) \quad (31)$$

The following important flow properties were derived as simple functions of S from Eqs (14) and (31) and the definitions of S_θ and S :

$$\frac{V}{V_0} = \frac{[(1/S_0)+\tan\phi]}{[(1/S)+\tan\phi]} \quad (32)$$

$$\frac{V_\theta}{V_0} = \left[\frac{1}{S_0}+\tan\phi\right]N\cos^2\phi \quad (33)$$

$$\frac{E}{E_0} = \left[N\cos^2\phi + \frac{1}{1+S\tan\phi}\right](1+S_0\tan\phi) \quad (34)$$

Also, from Eq (4) and the definition of M_z,

$$\frac{T}{T_0} = \left(\frac{V_z}{V_{z0}}\frac{M_{z0}}{M}\right)^2 \quad (35)$$

$$\frac{P}{P_0} = \frac{V_z}{V_{z0}}\left(\frac{M_{z0}}{M}\right)^2 \quad (36)$$

where the zero subscript designates the parameter values at the channel inlet The initial azimuthal velocity was assumed zero Equation (33) shows that V_θ increases linearly with distance along the channel This resulted since the azimuthal accelerating force equal to JB is constant for constant J_z and B

In addition to the foregoing flow properties, an integrated conversion efficiency was defined as

$$\eta = \frac{\int_0^z (\mathbf{J}\times\mathbf{B})_z V_z A\,dz}{\int_0^z \mathbf{E}\,\mathbf{J}A\,dz} \quad (37)$$

It represents the ratio of axial body force work to electrical energy input Substituting the axial component of Eq (2) for the numerator and Eq (3) for the denominator and using the fact that $\rho V A = \text{const}$ yielded

$$\eta = \frac{\frac{1}{2}(V_z^2 - V_0^2) + \int_0^z RT\frac{dP}{P}}{h_T - h_{T0}} \quad (38)$$

It should be noted that the present analysis doesn't consider the possibility of converting the azimuthal velocity[17] and the static enthalpy into axial velocity in a suitable nozzle Either would improve the Hall propulsor performance by increasing the specific impulse However, the maximum specific impulse, considering the plasma as a perfect gas, is $(2H_T/g)^{1/2}$ for any gasdynamic propulsor

Flow Regimes

The axial distributions of S and M were determined from the numerical integration of Eqs (29) and (30) Inserting these into Eqs (32–36) gave the remaining flow properties However, many characteristics were determined without actually solving these equations Thus, given M, the signs of dV/dz, dS/dz, and $(d/dz)M$ depend on the signs of the bracketed terms in Eqs (21, 29, and 30), respectively For supersonic acceleration these must be negative Limiting values for S and M_z are obtained when the foregoing derivatives and, consequently, the bracketed terms are zero Thus

$$S^2 - \frac{1}{\gamma}\tan\phi S + \frac{\gamma-1}{\gamma} = 0 \quad (39)$$

for $(d/dz)S = (d/dz)V_z = 0$, and

$$\left(1+\frac{\gamma-1}{2}M^2\right)S^2 - \frac{\gamma+1}{2\gamma}\tan\phi S + \frac{\gamma-1}{2\gamma}(1+\gamma M_z^2) = 0 \quad (40)$$

for $(d/dz)M = 0$ Similar relations can be obtained for $dP/dz = 0$ and $dT/dz = 0$ from Eqs (26) and (27), respectively

The magnetogasdynamic flow regimes that resulted from solving Eqs (39) and (40) are shown in Figs 3–5 for $\gamma = \frac{5}{3}$ Figure 3 gives the solution of Eq (39) in terms of S as a function of $\tan\phi$ This curve represents $(d/dz)V_z = dS/dz = 0$ for $M_z \neq 1$, or a sonic transition Thus, for supersonic flow, there are minimum and maximum values of S between which acceleration is possible and external to which the flow decelerates In addition, there is a minimum value of $\tan\phi = 2[\gamma(\gamma-1)]^{1/2}$ below which a supersonic flow can only decelerate

At large values of $\tan\phi$, S becomes asymptotic to

$$S_{\min} = \frac{1}{2\gamma}\tan\phi\left\{1 - \left[1 - \frac{4\gamma(\gamma-1)}{\tan^2\phi}\right]^{1/2}\right\} \to \frac{\gamma-1}{\tan\phi} \quad (41)$$

$$S_{\max} = \frac{1}{2\gamma}\tan\phi\left\{1 + \left[1 - \frac{4\gamma(\gamma-1)}{\tan^2\phi}\right]^{1/2}\right\} \to \frac{\tan\phi}{\gamma} \quad (42)$$

Inserting these limits for S_0 and S, respectively, in Eq (32)

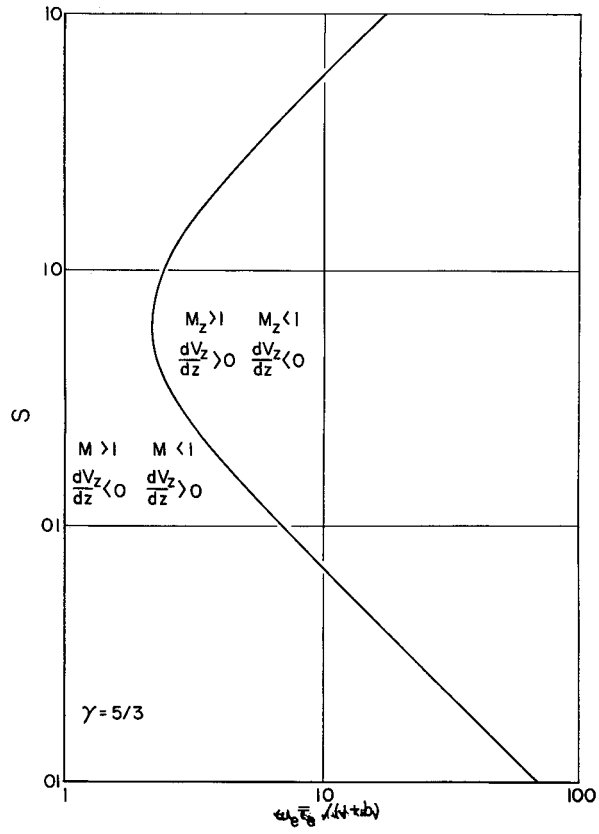

Fig 3 Regions of acceleration for constant area Hall propulsor

yielded

$$\frac{V_z}{V_0} = \frac{\gamma}{\gamma - 1} \frac{\tan^2\phi}{\gamma + \tan^2\phi} \tag{43}$$

which indicated that the maximum axial velocity increase, obtained as $\tan\phi \to \infty$, is $\gamma/(\gamma - 1)$ for a Hall propulsor with radial magnetic and axial electric fields This limit is the same for a Faraday propulsor [12] Higher ratios can be attained by staging the Hall propulsor, as discussed in a later section Figure 4 is a plot of Eq (40) for $\gamma = \frac{5}{3}$ and $\tan\phi = 15$ Within this curve, electromagnetic body force effects are greater than joule heating effects Therefore, the Mach number of an initially supersonic flow increases External to this curve the reverse is true The values of S at $M = 1$ are the limiting values in Fig 3 for $\tan\phi = 15$ The major feature of Fig 4 is the maximum Mach number for supersonic flow For $\tan\phi = 15$ it is approximately 4. As $\tan\phi$ increases $(M)_{max}$ also increases, as shown in Fig 5 Similarly, it is greater for a diverging rather than a constant area channel The practical significance of $(M)_{max}$ is that large

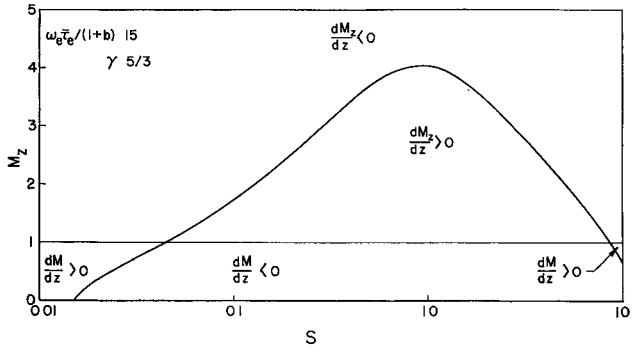

Fig 4 Regions of increasing Mach number for constant area Hall propulsor

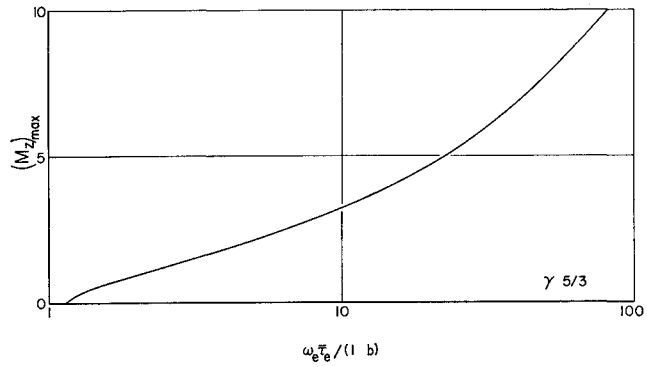

Fig 5 Maximum Mach number as a function of Hall parameters for a constant area propulsor

specific impulses are synonymous with large final static temperatures

Another important result deduced from Figs 3 and 4 concerned the sonic transition point The singularity at $M_z = 1$ of Eqs (29) and (30), in conjunction with the physical impossibility of infinite derivatives, insures that Eq (39) must be satisfied at the sonic transition point [11] Thus S at the sonic transition is found from Fig 3 as a function of $\tan\phi$ The two solutions for S correspond to the conditions

$$(S)_{min}: \quad dM/dz > 0 \qquad dS/dz > 0 \qquad dV_z/dz > 0$$

$$(S)_{max}: \quad dM/dz < 0 \qquad dS/dz \lesseqgtr 0 \qquad dV/dz \lesseqgtr 0$$

where $(S)_{min}$ corresponds to transition from subsonic to supersonic flow and $(S)_{max}$ corresponds to transition from supersonic to subsonic flow From a propulsion viewpoint, a good starting point is at $M = 1$ with $S = (S)_{min}$ to take advantage of the large region of acceleration with increasing Mach number

Numerical Results

Equations (29) and (30) were numerically integrated using the IBM 704 digital computer Initial conditions were chosen as $M = 1$ and $S = (S)_{min}$, thus avoiding the problem of a sonic transaction in an MGD flow The derivatives of S and M at $M = 1$ were evaluated from Eqs (29) and (30) by the method of L'Hospital These initial derivatives, given by

$$\frac{dM_z}{dz'} = -\gamma N \cos^2\phi \frac{(1 + \tan\phi S_{min})}{S_{min}} \left(S_{min} - \frac{\tan\phi}{2\gamma}\right) \tag{44}$$

$$\frac{dS}{dz'} = \frac{2\gamma}{\gamma + 1} N \cos^2\phi \left(\frac{1 + \tan\phi S_{min}}{S_{min}}\right)\left[\frac{\gamma - 1}{2} \times (1 + S_{min}^2) - S_{min}(1 + \tan\phi S_{min})\left(S_{min} - \frac{\tan\phi}{2\gamma}\right)\right] \tag{45}$$

agree with the conditions for a sonic transition since, from Eq (39),

$$S_{min} < \tan\phi/2\gamma$$

Figure 6 for $\tan\phi = 5$ and Fig 7 for $\tan\phi = 15$ show the various flow characteristics as functions of the magnetic interaction parameter, defined by Eq (25), which is directly proportional to propulsor length Figure 8 is a plot of the flow path in terms of M and S for $\tan\phi = 15$ In addition to the limiting Mach number curve from Eq (30) and Fig 4, Eqs (26) and (27) for $dP/dz = 0$ and $dT/dz = 0$, respectively, were plotted Thus, a comparison of Figs 7 and 8 permits an explanation of the peaks and valleys in the flow characteristics As an example, the local peak in the static temperature variation corresponds to the first intersection of the flow path with the $dT/dz = 0$ curve in Fig 8, whereas the valley corresponds to the second intersection Similarly,

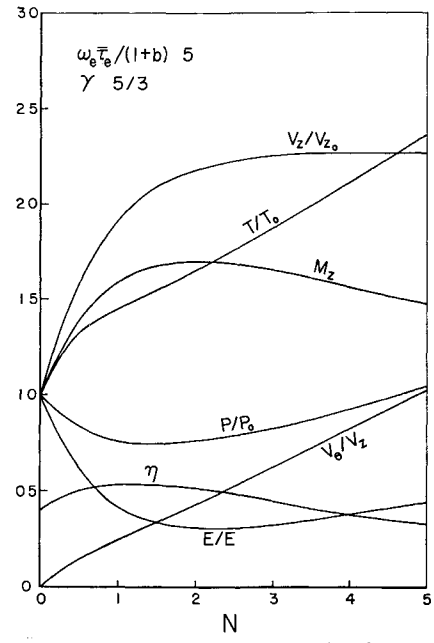

Fig 6 Hall propulsor characteristics for tanϕ = 5

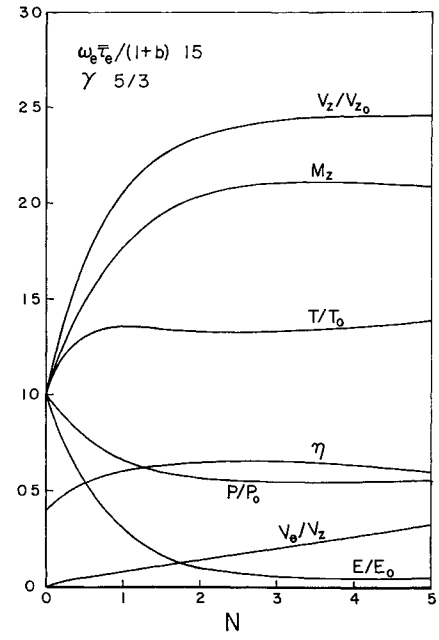

Fig 7 Hall propulsor characteristics for tanϕ = 15

peak Mach number corresponds to the flow path crossing the $(d/dz)M = 0$ curve The propulsor lengths required to attain peak efficiency, peak Mach number, or the asymptotic axial velocity are small compared to the length required to choke the flow Comparing Figs 6 and 7 shows that the maximum axial velocity increases with tanϕ as predicted by Eq (43) More significant, from a propulsor design viewpoint, is the increase in conversion efficiency with tanϕ It can thus be concluded that tanϕ should be as large as possible

It should be noted that, assuming a constant degree of ionization rather than constant electrical conductivity, Cann et al [23] were able to show that S is constant for constant β and the velocity ratio is infinite at the maximum Mach number

Staging

From Fig 7 the peak axial Mach number, for tanϕ = 15, is approximately 2 1 compared to the maximum attainable of 4 from Fig 5 As a consequence, it is possible to increase the basic Hall propulsor exit velocity from 2 5 V_0 by staging without large static temperature increase Although there are numerous staging schemes, the most reasonable, particularly with respect to minimizing the over-all static temperature increase, is to ricochet between the boundaries defining the region $dM/dz > 0$ in Fig 4 Thus, in the first stage, acceleration would begin at the minimum sonic transition point in Fig 4 and end when the boundary $dM/dz = 0$ was reached at $M_z = 2\,1$ The second-stage current would be adjusted, via the voltage drop across this stage, such that the initial S is the smaller value on the $dM/dz = 0$ curve at $M = 2\,1$ Similar current adjustments would be made for succeeding stages Since the change in S decreases as the maximum value of M is approached, the velocity ratio across each stage decreases in accordance with Eq (32) Preliminary calculations showed that after 10 stages the over-all axial velocity ratio increased to approximately 11, whereas the axial Mach number increased to 3 7

Plasma Properties

The results of the present analysis indicated that the ratio of the Hall parameter $\omega_e\bar{\tau}$ to one plus the "ion slip" parameter b should be large to maximize the velocity ratio across each stage From Eq (7),

$$b = 2f^2(\omega\bar{\tau})^2[\omega_i\tau_{ia}/\omega\bar{\tau}] \quad (46)$$

where the bracketed quantity is independent of $\omega\bar{\tau}$ for a specified gas at constant temperature and electron energy Thus, tan$\phi = \omega\bar{\tau}/(1+b)$ is a function of $\omega\bar{\tau}$ Its maximum value occurs when $b = 1$ or $(\omega\bar{\tau})(\omega_i\tau_{ia}) = \frac{1}{2}$ For a slightly ionized plasma, since $\tau_a \ll \tau_i$, $\omega\bar{\tau} \approx \omega\tau_{ea}$

The conditions of pressure, temperature, electron energy, and magnetic field for which tanϕ is a maximum were determined for argon in the following manner From the probability of elastic electron-atom data given by Brown[18] as functions of electron energy, $\omega\tau_a$ was computed from

$$\omega\tau_a = \frac{10\,865}{U^{1/2}P_c}\left(\frac{BT}{P}\right) \quad (47)$$

and plotted in Fig 9 It should be noted that n depends on the value of BT/P required to maximize tanϕ The dashed curve corresponds to the rigid elastic sphere model for $BT/P = 10^n$, for which

$$(\omega\tau_{ea})_s = \frac{3\,91}{(\sigma_a)}\left(\frac{BT}{P}\right)\frac{1}{U^{1/2}} \quad (48)$$

As is readily seen, the rigid sphere model deviates widely in certain ranges of electron energy

The ratio of ion cyclotron frequency to ion-atom collison frequency, assuming thermal equilibrium between neutrals and ions and a Maxwellian distribution for the ion velocity,

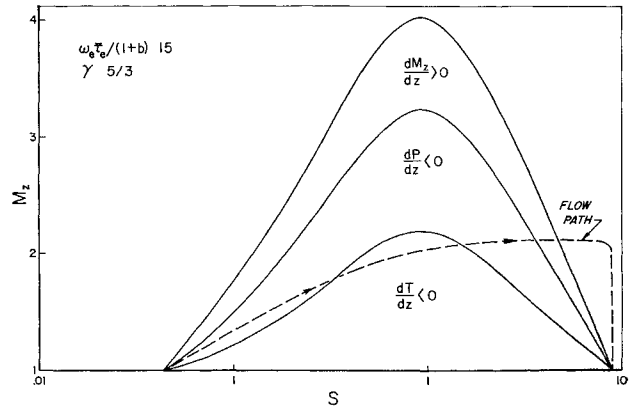

Fig 8 Flow path for supersonic acceleration at tanϕ = 15

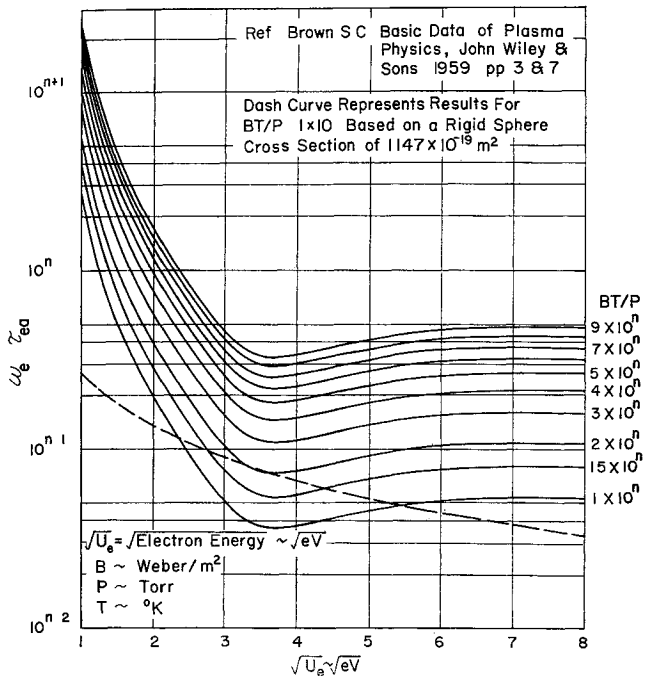

Fig 9 Hall parameter for slightly ionized argon plasma

is given by

$$\omega_i \tau_{ia} = \frac{6\,8649}{Q_{ia} T^{1/2}} \left(\frac{BT}{P} \right) \frac{1}{M} \qquad (49)$$

The ion-neutral cross section was computed from viscosity data[19 20] following Cann [21] Thus, combining Eqs (47) and (49) yielded Fig 10, which gives the relation between bulk plasma temperature, electron energy, and the parameter BT/P The ranges of electron energy and plasma temperatures were chosen to permit investigations of nonequilibrium plasmas [22]

Concluding Remarks

The results of the preceding one-dimensional analysis of the coaxial constant area Hall propulsor with radial magnetic field and axial electric field showed that the maximum attainable velocity ratio is 2 5 for a slightly ionized gas This value can be approached at moderate values of the parameter $\tan\phi = \omega \bar{\tau}_e/(1 + b)$ In addition, the maximum attainable Mach number increases with $\tan\phi$ It was further demonstrated that $\tan\phi$ is a function of $\omega_e\bar{\tau}$ and reaches its peak at $b = 1$ In general, $\tan\phi$ increases with increasing molecular weight However, since the initial plasma velocity at sonic conditions decreases with increasing molecular weight, the choice of a suitable propellant to maximize the final velocity at a specified static temperature requires a more detailed evaluation than presented in this discussion

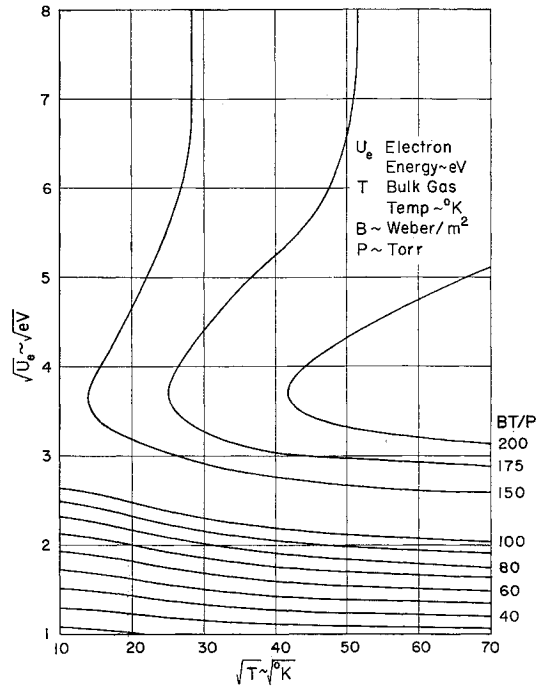

Fig 10 Conditions for optimum $\omega_e\bar{\tau}_e/(1 + b)$ for slightly ionized argon plasma

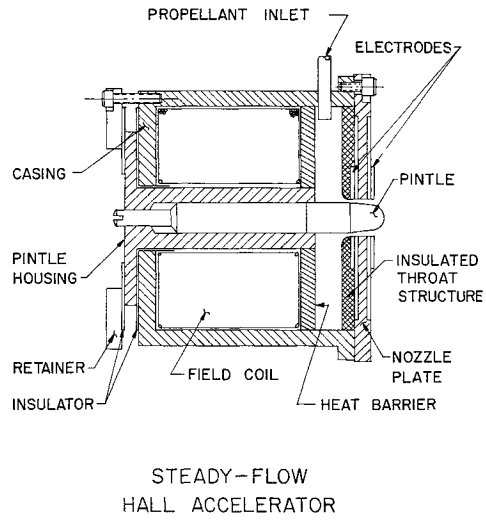

Fig 11 Schematic of Hall propulsor experimental model

For a given propellant, the final plasma velocity, and therefore the propulsor specific impulse, can be increased by staging, using a variable rather than a constant area channel, expanding the flow in a suitable nozzle to convert the azimuthal velocity component and/or the static enthalpy into axial velocity, or using a combination of these techniques

The single-stage experimental model, shown in Fig 11, was designed and fabricated to verify the predictions of this analytical investigation Experimentation is currently being conducted using a radio frequency generated argon plasma for which the pintle and casing serve as electrodes The radial magnetic field is provided by a plunger-type electromagnet in which the magnetic path is axial through the pintle and radial through the MGD interaction zone The return loop is through the propulsor casing D c power electrodes are circular disks secured to and insulated from the upstream and downstream faces of the nozzle plate The MGD interaction zone is a slightly diverging rather than a constant area channel to minimize fabrication problems associated with small radial gaps and to counteract the adverse effects of fluid friction

In conclusion, it may be stated that the results obtained in this investigation were sufficiently encouraging to warrant further analytical and experimental evaluation of the potential of the Hall propulsor to efficiently fill the specific impulse gap shown in Fig 1

References

[1] Jack, J R , "Theoretical performance of propellants suitable for electrothermal jet engines," NASA TN D-682 (March 1961)

[2] Kaufman, H R , "The electron bombardment ion engine," *Advanced Propulsion Concepts* (Gordon and Breach, New York, 1963), pp 3–18

[3] Mickelsen, W R , "Comparative performance of electrostatic rocket engines," IAS Preprint 62-74 (1962)

[4] Sutton, G W and Gloersen, P "Magnetohydrodynamic

power and propulsion, *Magnetohydrodynamics*, edited by A B Cambel, T P Anderson, and M M Slawsky (Northwestern University Press, Evanston Ill , 1962), pp 243–268

[5] Demetriades, S T and Ziemer, R W , "Energy transfer to plasmas by continuous Lorentz forces," *Magnetohydrodynamics*, edited by A B Cambel, T P Anderson, and M M Slawsky (Northwestern University Press, Evanston, Ill 1962), pp 185–205

[6] Bodoia, J R , Lenn, P D , Ward, D L , and Demetriades, S T , Three-fluid non equilibrium plasma accelerators," AIAA Preprint 63047 (March 1963)

[7] Hess, R V "Experiments and theory for continuous steady acceleration of low density plasmas, *Proceedings of the XIth International Astronautical Congress* (Springer, Stockholm, 1960), pp 404–411

[8] Sevier, J R , Hess, R V , and Brockman, P , "Coaxial Hall current accelerator operating at forces and efficiencies comparable to conventional crossed-field accelerators," ARS J **32**, 78 (1962)

[9] Hess, R V , Burlock, J , Sevier, J R , and Brockman, P , "Theory and experiments for the role of space charge in plasma acceleration," *Symposium of Electromagnetics and Fluid Dynamics of Gaseous Plasma* (Polytechnic Press of the Polytechnic Institute of Brooklyn, Brooklyn, N Y , 1962), pp 269–305

[10] Brandmaier, H E , Durand, J L , Gourdine, M C and Rubel, A , "An investigation of a one kilowatt Hall accelerator," AIAA Preprint 63046 (March 1963)

[11] Shapiro, A H , *The Dynamics and Thermodynamics of Compressible Fluid* (Ronald Press Co , New York, 1953), Vol 1, pp 219–262

[12] Yoler, Y A , "A review of magnetohydrodynamics," *Plasma Physics* edited by J R Drummond (McGraw-Hill Book Co , Inc , New York, 1961), pp 174–177

[13] Resler, E L , Jr and Sears, W R , 'The prospects for magnetoaerodynamics," J Aeronaut Sci **25**, 235–245 (1958)

[14] Hess, R V , Fundamentals of plasma interaction with electric and magnetic fields" *Plasma Physics and Magnetohydrodynamics in Space Exploration*, NASA SP-25 (December 1962)

[15] Ellis, M C , Jr , "Survey of plasma accelerator research," *Plasma Physics and Magnetohydrodynamics in Space Exploration*, NASA SP-25 (December 1962)

[16] Cowling, T G , *Magnetohydrodynamics* (Interscience Pub lishers, Inc , New York, 1957), pp 105–108

[17] Patrick, R M and Powers, W E , "Plasma flow in a magnetic arc nozzle," *Advanced Propulsion Concepts* (Gordon and Breach, New York, 1963), pp 115–136

[18] Brown, S C , *Basic Data of Plasma Physics* (John Wiley and Sons, Inc , New York, 1959), pp 3, 7

[19] Svehla, R A , "Estimated viscosities and thermal conductivities of gases at high temperatures," NASA TR R-132 (1962)

[20] Amdur, I and Mason, E A , "Properties of gases at very high temperatures," Phys Fluids **1**, 370 (1958)

[21] Cann, G L , "Energy transfer processes in a partially ionized gas," Memo 61, Hypersonic Research Project, Grad Aeronaut Lab , Calif Inst Tech (June 1961)

[22] Gourdine, M C , "Non-equilibrium RF plasmas for magnetogasdynamic energy conversion," Symposium on Magnetoplasmadynamic Electrical Power Generation, King s College, University of Durham, England (September 1962), Paper 35

[23] Cann, G L , Ziemer, R W , and Marlotte, G L , "The Hall current plasma accelerator," AIAA Preprint 63011 (March 1963)